

ESTIMATION OF LATERAL-DIRECTIONAL PARAMETERS FROM FLIGHT DATA USING NEURAL NETWORKS

by
SUNIL KHUSCHANDANI



DEPARTMENT OF AEROSPACE ENGINEERING

ESTIMATION OF LATERAL-DIRECTIONAL PARAMETERS FROM FLIGHT DATA USING NEURAL NETWORKS

A Thesis Submitted
In Partial Fulfillment of the Requirements
for the Degree of
MASTER OF TECHNOLOGY

by
Sunil Khubchandani



to the
DEPARTMENT OF AEROSPACE ENGINEERING
INDIAN INSTITUTE OF TECHNOLOGY KANPUR

ACKNOWLEDGEMENT

I express my deep sense of gratitude to my esteemed teachers and thesis supervisors, Dr. B.C. Dasgupta and Prof. A.K. Ghosh for their invaluable guidance, constructive criticism and persistent encouragement throughout this work. I shall always remain indebted to them for the precious time they have spent for me and the patience with which they always enlightened my path.

With all sincerity, I thank Dr. P.K. Saha, the professor of Electrical Engg. Deptt. for his guidance and all the facilities he provided me for finishing my work in time.

I have no words to express my thanks to my parents and my youngsters who have been constant source of inspiration to me. I wish to thank all my friends and well wishers who made my stay at I.I.T.K. memorable and pleasant.

SUNIL G K.

DEDICATED TO
MY FAMILY

MR. DE. SUBRAMANIAM

MRS. KAMLA DEVI SUBRAMANIAM

YASWALI, Noida AND Hrish

ABSTRACT

Application of Fast Forward Neural Network (FFNN) in Aerospace Engineering problem is one of the current topics of interest. The FFNNs do not require an a priori model of aircraft for modeling, and provide a black - box type of model of the aircraft by mapping available network inputs to chosen network outputs. The present thesis deals with modeling of aircraft lateral-directional dynamics through FFNNs and application of recently proposed Delta-method for the estimation of aircraft stability and control derivatives (parameters). For modeling aircraft motion variables and the control inputs are used as the input file while aerodynamic force or moment coefficients are used as the output file for training FFNN. For the purpose of parameter estimation, the trained FFNN is now presented with suitably modified input file and the corresponding predicted output files of force and moment coefficients are obtained. Delta's Interpretation and processing of these input-output files results in estimated values of the parameters. The method is verified on lateral-directional simulated flight data. A detailed study has been carried out to show how the accuracy of estimates gets affected when flight data corresponding to various types and forms of aircraft and/or rudder control inputs are analyzed. It is shown that the combination of aircraft and rudder applied in certain sequential form tends to better estimates. Finally, it is also shown that the Delta-method is quite robust and can be used for parameter estimation even if flight data contains measurement noise.

CONTENTS

ABSTRACT

List of Figures

List of Symbols

CHAPTER	TITLE	Page No
1	INTRODUCTION	1
2	FEED FORWARD NEURAL NETWORKS	9
3	SIMULATED FLIGHT DATA GENERATION AND THE METHOD USED	19
4	RESULTS AND DISCUSSION	25
5	CONCLUSION AND RECOMMENDATIONS	26
	REFERENCES	29
	TABLES	42
	FIGURES	50

LIST OF FIGURES

Serial Number	Page Number
1. Figure of a aircraft	5
2. Figure of FFGH with two hidden layers	56
3. Figure Showing Aircraft Axes System	51
4. Three Types Of Control Input Forms	52
5. Figure of Pulse type control input (case II)	53
6a. Figure of multistage 2-2-1-1 aircraft input signal (case VIII)	54
6b. Figure of multistage 2-2-1-1 rudder input signal (case VIII)	55
7a. Comparison Of Actual, Trained and Estimated Response Of Rolling Moment Coefficient (C_{lr})	56
7b. Comparison Of Actual, Trained and Estimated Response Of Yawing Moment Coefficient (C_{ly})	57
7c. Comparison Of Actual, Trained and Estimated Response Of Force Coefficient Along Y-axis (C_{ly})	58
8a. Histograms For Estimated Parameters C_{lp} , C_{lr} , C_{lp} , $C_{l\dot{\alpha}}$ and $C_{l\dot{\alpha}}$	59
8b. Histograms For Estimated Parameters C_{ay} , C_{ay} , C_{ay} , $C_{y\dot{\alpha}}$ and $C_{y\dot{\alpha}}$	60
8c. Histograms For Estimated Parameters C_{yp} , C_{yp} , C_{yp} , $C_{y\dot{\alpha}}$ and $C_{y\dot{\alpha}}$	61

LIST OF SYMBOLS

SYMBOLS

C_D	rolling moment coefficient
C_L	rolling control coefficient
C_p	force coefficient along X-axis
E	error cost function
I_{ax}	moment of inertia about x-axis kg-m^2
l	reference area m^2
U_1	velocity, m/sec
u	span, m
f	radisson sigmoidal activation function
m	aircraft mass, kg
n_1	number of nodes in input layer
n_2	number of nodes in hidden layer
n_3	number of nodes in output layer
p	roll rate, rad/sec
r	yaw rate, rad/sec
s	half the span, m
w	weight matrix between two layers
\hat{y}	estimated output
z	desired output
θ	sideslip angle, deg or rad
δ_a	aileron deflection, deg
δ_r	rudder deflection, rad
k	logistic gain or slope factor
η	learning rate parameter

Superscript

\cdot	derivative with respect to load
T	transpose of matrix

Stability and Control Derivatives

$$C_{\dot{\delta}_B} = \partial C_F / \partial (\dot{\delta}_B / 20^\circ \text{s}^{-1}) \quad , \quad C_{\dot{\delta}_B} = \partial C_N / \partial (\dot{\delta}_B / 20^\circ \text{s}^{-1}) \quad , \quad C_{\dot{\delta}_B} = \partial C_Y / \partial (\dot{\delta}_B / 20^\circ \text{s}^{-1}) \quad ,$$

$$C_{\dot{\delta}_F} = \partial C_F / \partial (\dot{\delta}_F / 20^\circ \text{s}^{-1}) \quad , \quad C_{\dot{\delta}_F} = \partial C_N / \partial (\dot{\delta}_F / 20^\circ \text{s}^{-1}) \quad , \quad C_{\dot{\delta}_F} = \partial C_Y / \partial (\dot{\delta}_F / 20^\circ \text{s}^{-1}) \quad ,$$

$$C_{\dot{\delta}_B} = \partial C_F / \partial \dot{\delta}_B \quad , \quad C_{\dot{\delta}_B} = \partial C_N / \partial \dot{\delta}_B \quad , \quad C_{\dot{\delta}_B} = \partial C_Y / \partial \dot{\delta}_B \quad ,$$

$$C_{\dot{\delta}_B} = \partial C_N / \partial \dot{\delta}_B \quad , \quad C_{\dot{\delta}_B} = \partial C_N / \partial \dot{\delta}_B \quad , \quad C_{\dot{\delta}_B} = \partial C_Y / \partial \dot{\delta}_B \quad ,$$

$$C_{\dot{\delta}_F} = \partial C_F / \partial \dot{\delta}_F \quad , \quad C_{\dot{\delta}_F} = \partial C_N / \partial \dot{\delta}_F \quad , \quad C_{\dot{\delta}_F} = \partial C_Y / \partial \dot{\delta}_F$$

INTRODUCTION

The process of estimating numerical values of aerodynamic stability and control derivatives (parameters) from flight test data is termed as Parameter Estimation. The mathematical model representing airplane dynamics requires accurate values of these parameters. Such mathematical models are useful for verification of stability augmentation system (SAS) and in-flight controllers.

Three distinct approaches for estimating these stability and control derivatives are

- (i) Theoretical Methods
- (ii) Wind Tunnel Testing
- (iii) Flight Testing

At initial design stages of aircraft design, theoretical methods¹⁻³ provide the only immediate way of obtaining the aircraft parameters. However, the accuracy of such theoretical estimates being not so high, there is need to verify these estimates with those obtained from wind tunnel testing and flight testing. Wind tunnel methods although improve accuracy of estimates of parameters, they are time consuming and expensive. Further, simulation of tested surfaces, power effects and stringent flight conditions are difficult to simulate satisfactorily. Wind tunnel estimates also suffer from discrepancies due to interference effects of support system, wall effects, turbulence level etc. It is, therefore, desirable that the wind tunnel estimates be corroborated with estimates from actual flight test data.

Three popular methods to estimate stability and control derivatives from flight test data are as follows :

- (i) Least Squares Method
- (ii) Output Error Method
- (iii) Maximum Likelihood Method

The principle of least squares is used in Least Squares Method. The error gets minimized with respect to unknown parameters in each of the equations. Its advantages include computational simplicity, non-iterative nature and applicability to both linear as well as nonlinear models. However this method can not be applied if all the states are not measured accurately and gives poor results if measurements are noisy. Thus in order to get accurate results ample efforts are required for data reconstruction and smoothing. Some times these data processing tasks are more complicated than the task of parameter estimation itself. The errors between the measured and model response produced by identical inputs is minimized by Output Error Method. The method assumes that there exist no modeling errors. The method processes the measured value while assuming the model representation of given system to be exact. A comprehensive survey of these methods is reported by Moss and Hill⁴. The methods like analog modeling⁵, Newton-Raphson Method⁶, Modified Newton-Raphson Method⁷ etc. fall in this category.

Maximum likelihood⁸ estimates are those for which the observed value would be the most likely to occur. The main advantage of this method is that estimated parameters are asymptotically

approximation which can collectively model any nonlinear relationship between the inputs and the outputs.

ANN can only operate with given input-output data. Some networks require only input variables and are called as auto associative networks while others require input-output pairs and are called as hetero associative networks.

Nodes or neurons are the sites where all the computations are performed. Figure 1 illustrates the most common type of neuron. Each neuron collects information from abutting connections and produces single output value. ANNs also consist of edges/connections between the nodes which not only allow information to flow in particular defined direction but also assign weight to the information. Such connection weights are termed as synaptic weights. These weights are adjusted in accordance to a well defined algorithm which helps to capture knowledge within the network.

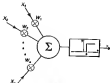


Figure 1 | Single Neuron

Due to the above properties, ANNs are widely preferred for mapping any nonlinear relationship between the input and output. It can be stated that it is a "black box model structure" because functional relationship between the input and output is not explicitly known.

There are several types of ANNs, but only two of them have successfully found application in the field of aircraft system identification. These are -

(a) Feed Forward Neural Network (FFNN)

(b) Recurrent Neural Networks (RNN)

FFNNs tend to a black box model in which no physical significance can be added to either network structure or to the network weights.¹²⁻¹⁴ RNNs have fixed structure and possess fixed number of nodes, equal to number of unknown parameters.

FFNNs have neurons arranged in layers like directed graphs and thus are static in nature. RNNs are dynamic neural networks incorporating an output feedback. In recent paper Karl and Jorgensen¹⁵ have shown suitability of RNNs to state space modeling and thereby demonstrated their applicability to explicitly estimate aircraft parameters. However as pointed by authors,¹⁶ RNNs have only a limited scope for aircraft identification applications and it is the FFNNs which may prove to be more flexible and thereby have higher potential for future applications for modeling aircraft dynamics and aircraft parameter estimation.

Presently, system identification has been re-oriented by many

researchers using ARMA^{[2]-[3]}. Significant contributions in this direction have been made by Han^[4], Yousif and Jiang^[5], Ranaivosoa and Jategaonkar^[6], Erol and Jategaonkar^[7], and Laine and Strong^[8]. Han^[3] dealt with use of FFTs to represent aircraft aerodynamics. Yousif et al^[5] demonstrated the feasibility of neural modeling approach to establish a nonlinear aerodynamic model that is suitable to flight test data processing. Ranaivosoa and Jategaonkar^[6] have studied various aspects of FFTs modeling and its applicability to real flight data. Erol and Jategaonkar^[7] have shown use of FFT for aircraft parameter estimation. Laine and Strong^[8] have shown accurate modeling of aerodynamic coefficients using a system identification model composed of an extended Kalman filter for state and force estimation and a computational neural network for aerodynamic model.

In a recent paper Balafoutis et al^[9] have proposed two new methods for estimation of airplane parameters using FFTs. The proposed methods are called Delta-Method and Zero-Method. Both methods have been validated on simulated flight data generated for longitudinal dynamics of an example aircraft. Out of these two Delta Method was shown to be more reliable, consistent and robust. We have therefore chosen Delta method for present study wherein its applicability to extract lateral-directional stability and control parameters from flight data is explored. Specifically following aspects of application of FFTs to aircraft lateral-directional dynamics are dealt with:

(a) Aerodynamic modeling of lateral-directional dynamics using

FFNN) wherein force and moment coefficients C_L, C_D, C_Y are mapped to measured motion variables p, r, β and control inputs δ_a, δ_r . Various aspects about identifying variable FFNN structure and associated network parameters like learning rate, momentum rate, slope etc. are studied.

(vi) Application of Determined for mapping internal-directional parameters from simulated flight data for an example aircraft is demonstrated. A detailed study has been carried out to show how accuracy of estimates is affected by the type of control input used for generating flight data. Results are also presented to indicate the effect of measurement noise present in the simulated flight data on the accuracy of estimates.

The layout of the present work is as follows:

After introduction in chapter one, details of FFNN and backpropagation algorithms are given in chapter two. Chapter three deals with the method used for parameter estimation and various aspects about the generation of simulated flight data. Chapter four consists of descriptive study of the results obtained. Lastly, chapter five deals about the conclusions drawn on the basis of results obtained and also about the recommendations for future work.

CHAPTER 2	
FEED FORWARD NEURAL NETWORKS	
2.1 General	
2.2 Backpropagation	
2.2.1 Initialization of Weights	
2.2.2 Forward Propagation	
2.2.3 Backward Learning Algorithm	
2.3 Modeling, Prediction And Software	
Parameters of FFNN	

FIXED FORWARD NEURAL NETWORKS

3.1 General

FFNNs are fully layered perceptrons consisting of an input layer, an output layer and one or more hidden layers. The number of neurons/nodes in the input layer and the output layer are determined respectively by the number of input and output variables while the number of neurons in the one hidden layer(s) is decided by the complexity of the problem. Figure 2 shows a general schematic picture of FFNN with two hidden layers consisting of many neurons.

FFNNs are static and characterized by unidirectional flow of variables i.e. the inputs are propagated through the hidden layers to the output layer. Each node in the input/output or hidden is connected to each node in the next layer/layer(s) the hidden or the output through a connective weight. Every node in the input layer and the hidden(s) layer is biased. The nodes in the hidden layer(s) and the output layer have a nonlinear activation function, e.g. sigmoidal or hyperbolic tangent function. The hidden nodes in FFNN have good approximation capability and thereby allow the network to build a model of arbitrary complexity between the input(s) and the output(s).

For specific case of aircraft lateral-directional dynamics the input variables to the network are the motion variables p, q, r and the aircraft control input signals $\delta_a, \delta_r, \delta_s$ while the output variable is aerodynamic force or moment coefficient i.e.

average moment coefficient(C_{α}), or rolling moment coefficient(C_{α}), or force coefficient along y-axis(C_y). Figure 3 shows body fixed axes system. The known input/output data is first used to train the network. The predicted output values of C_1, C_2, C_3 are compared with the corresponding known values of C_1 or C_2 or C_3 and the errors are backpropagated using a method called the back propagation algorithm (BPA). This process results in updating of network's connection weights. The training of the network is continued till the mean square error (MSE), defined as follows, is less than the prescribed value.

Mean square error (MSE) defined by equation (1) is used to test the convergence. The influence parameters are varied until the MSE is within the defined limit. Mean square error can be expressed as

$$MSE = \frac{1}{N_m} \sum_{k=1}^N \sum_{j=1}^m (y_j(k) - \hat{y}_j(k))^2 \quad (1)$$

where, N is the number of data points, m is the number of input variables, y is the desired or measured response and \hat{y} is the estimated response of the network.

The details of BPA and forward propagation in RNN are discussed next.

2.2 Backpropagation Algorithm (BPA)

Backpropagation⁸ is a simple iterative gradient descent algorithm. The essential idea behind the BPA, which is widely

used for training multi-layered perceptrons , is to view the error function as a function of network weights or parameters and to perform gradient descent in the weight parameter space to search for a minimum error between desired and estimated value . In this method , weights are updated incrementally so that , at each iteration a small step is taken in the negative direction of the error to make it small more rapidly

There are two common types of BPN learning algorithms

1 Batch or Simple BPN

2 Sequential or Recursive BPN

The batch BPN updates the network weights after presentation of the complete training data set . Hence , a training iteration incorporates one sweep through all the training patterns

In case of recursive BPA , also called pattern learning , the network weights updated sequentially as the training data set is presented . The recursive BPA is more convenient and efficient as compared to the batch BPA .

A brief summary of the BPN algorithm for one hidden layerd FFNN is given below for completeness

2.2.1 Initialization of Weights

The input and output weight matrices of the network are initialized randomly . With reference to Figure 2 the order of weight matrices and weight vector is as follows :

Matrix/Vector	Symbol	Order of matrix/vector
6.1 weight matrix between input and hidden layers	w_1	$n_h \times n_i$
6.2 bias weight vector	w_{10}	$n_h \times 1$
6.3 weight matrix between hidden and output layer	w_2	$n_o \times n_h$
6.4 bias weight vector	w_{20}	$n_o \times 1$
where $n_i = n_h$ and n_o are the number of nodes in the input, hidden and output layers respectively		

2.2.2 Forward propagation

During the forward propagation, for a given input vector x_0 , the estimated output vector x_2 is computed

(i) Propagation from input layer to hidden layer

$$x_1 = w_1 \times x_0 + w_{10} \quad (2a)$$

$$x_1 = f(x_1) \quad (2b)$$

where x_1 is the vector of intermediate variables, x_1 is the vector node output at the hidden layer and f is the vector of nonlinear sigmoidal node activation function, defining the node characteristic

It should be noted that each component of the vector on left hand side corresponds to the respective component of the vector on right hand side for all the equations.

The sigmoidal function may be written as

$$f(x_1) = \frac{1}{1 + \exp(-x_1)} \quad i=1,2,\dots,n_h \quad (3)$$

where λ is the sigmoid gain or slope factor of the hidden layer activation function . All the nodes at any particular layer have , generally , the same slope factor

1.1 Propagation From hidden layers to output layer

$$x_2 = w_2^T y_1 + w_{20} \quad (1a)$$

$$y_2 = \sigma(x_2) \quad (1b)$$

where y_1 is the vector of intermediate variables , y_2 is the vector node output at the output layer and σ is the vector of nonlinear sigmoidal node activation function

Similarly , the sigmoidal function is then given by

$$f_i(x_2) = \frac{1}{1 + e^{-x_2/(kT_0)}} \quad \text{with } x_2 \quad (2)$$

2.2.2 Recurrent Learning Algorithm

The backpropagation learning algorithm is based on optimizing a suitably defined error cost function . At each point the local output error cost function , which is sum of squared errors , is given by

$$E_k = \frac{1}{2} \|x - u_2\|^2 = \frac{1}{2} (x - u_2)^T (x - u_2) \quad (3)$$

where k is the discrete time data index , x is the measured response vector , u_2 is the network estimated response vector and $u_2 = f(x - u_2)$ denotes the error .

Minimization of eq.(3), applying the steepest gradient descent method , also called delta rule , yields

$$\mathbf{w}_2^{k+1} = \mathbf{w}_2^k + \mu \cdot \mathbf{g} = \mathbf{g} \cdot \mathbf{E}_g / \mathbf{g} \cdot \mathbf{w}_2 \quad (7)$$

where $\mu > 0$ is learning rate parameter determining the speed of convergence, $\mathbf{g} = \mathbf{g}(\mathbf{E}_g / \mathbf{g} \cdot \mathbf{w}_2)$ is the gradient of error cost function with respect to \mathbf{w}_2 . A practical choice of learning rate parameter, μ , is necessary to ensure reasonable convergence rate.

Partial differentiation of eq.(6) with respect to the elements of weight matrix \mathbf{w}_2 and substitution of Eq. (6) & (4) yields gradient of the error cost function

$$(\mathbf{g} \cdot \mathbf{E}_g / \mathbf{g} \cdot \mathbf{w}_2) = -f'(\mathbf{y}_2) \cdot (\mathbf{z} - \mathbf{w}_2) \cdot \mathbf{u}_0^T \quad (8)$$

where $f'(\cdot)$ is the derivation of the output node activation function i.e. eq. (5)

Defining \mathbf{u}_{20} as

$$\mathbf{u}_{20} = f'(\mathbf{y}_2) \cdot (\mathbf{z} - \mathbf{w}_2) \quad (9)$$

and by adding momentum term to Eq. (7), the weight update rule for the output layer is obtained as

$$\mathbf{w}_2^{k+1} = \mathbf{w}_2^k + \mu \mathbf{u}_{20} \cdot \mathbf{u}_2^T + \Omega (\mathbf{w}_2^k - \mathbf{w}_2^{k-1}) \quad (10)$$

where Ω is momentum term.

Our relaxation of the gradient update i.e. of eq. (7), through the last term on the right hand side of eq. (9), called momentum term, helps to damp out the parasitic oscillations in the weight update, e.g., due to large value of learning rate, μ . Approximately, it amounts to increasing the learning rate from μ to $\mu / (1 - \Omega - \Omega)$ without magnifying the parasitic oscillations.

Similarly, the partial differentiation of eq. (4) with respect to \mathbf{w}_1 and substitution of eq. (3) & (2) yields

$$(\mathbf{g} \cdot \mathbf{E}_g / \mathbf{g} \cdot \mathbf{w}_1) = -f'(\mathbf{y}_1) \cdot \mathbf{u}_2^T \cdot \mathbf{u}_{20} \cdot \mathbf{u}_0^T \quad (11)$$

where $f'(x_{ij})$ is the derivative of hidden layer activation function $f(\cdot)$ as of eq. (2)

$$w_{jk}^{(2)} = f'(x_{ij}) w_{jk}^{(2)} + \eta \delta_j^{(2)} \quad (14)$$

The weight update rule for the hidden layer is given by

$$w_{ij}^{(2)} = w_{ij}^{(2)} + \eta \delta_j^{(2)} w_{ij}^{(2)} + \theta (w_{ij}^{(2)} - w_{ij}^{(2-1)}) \quad (15)$$

For the sigmoid function as eq (2) and eq (3) shown respectively as the hidden and output layer node activation function respectively, the derivatives $f'(x_1)$ and $f'(x_2)$ are given by

$$f'(x_1) = \frac{e^{-x_1} (1 - e^{-x_1})}{1 + e^{-x_1}} \quad (16)$$

It may be pointed out that the training algorithm is recursive, as stated above, the weights are updated sequentially for each time point using eqs (9) & (10)

From computational view point, the backpropagation algorithm (BPAB) requires

- (i) Computation of the hidden & output node activation function i.e. eqs (2) & (3) and eqs (5) & (6)
- (ii) Computation of the error cost function i.e. eqs (8) & (9)
- (iii) Computation of the derivatives of the node activation function in Eq (2) for hidden and output layer
- (iv) Computation of the new weights from Eqs. (11) & (12) until the desired accuracy is obtained

2.2 Modeling, Prediction And Influence Parameters of ITNN

As stated earlier problem solving using ITNN consist of two

phases namely i) learning or training phase and ii) prediction phase.

In modeling , learning or training phase procedure consists of presenting the known input and output data to network and adjusting the network weights using backpropagation algorithm (BPA). During this procedure network captures the functional relationship existing between the inputs and outputs (not necessarily in the same form as in the original physical model) in form of network weights . Once modeling or training is over and network weights and topology is frozen , the same data is passed through the network with the same topology to check for prediction capability of the network based on some convergence criteria (ACC) in the present study] .

There are several network parameters which affect the convergence rate . These influence parameters are

1. Number of Hidden Layers (H.L.)
2. Number of neurons in each hidden layer (n's.)
3. Learning Rate Parameter (η)
4. Momentum Rate Parameter (θ)
5. Number of iteration (N)
6. Initial Network Weights (R.S.)
7. Weight Limit
8. Logistic Gain or slope Factor (α)

Determination of optimal topology is a cumbersome job . It is hit and trial method which is like part science and part art . In standard literature on FFNN , some design rules have been proposed

for structure and parameters of FNN's for various applications. One has to still develop one's own set of thresholds by repeated trials of training the network for the problem at hand. We have found and recommended a set of values of influence parameters for mapping lateral-directional dynamics of an aircraft. These values are presented in chapter four.

CHAPTER 3
PARAMETER ESTIMATION METHOD
AND
SIMULATED FLIGHT DATA GENERATION

3.1 General

3.2 Data-set used

3.3 Simulated Data Generation

3.4 Equations of Motion

SIMULATED FLIGHT DATA GENERATION

3.1 General

In this chapter we first describe the salient features of Delta-method¹⁷ used for parameter estimation from flight data using Feed Forward Neural Networks. Next we outline the procedure used and types of simulated data generated for analysis via Delta-method. Details of the example airplane used and types of control inputs utilized for generating simulated flight data are also given. Flight data with and without pseudo measurement noise were prepared for analysis. Although real flight data for lateral-directional dynamics of an airplane were recently obtained and are being separately analyzed by others we did use the control input form used for real flight data to generate corresponding simulated flight data for analysis and comparison with the results obtained by others. Scarcity of time did not permit analysis of the complete real flight data to be included in the present work.

3.2 Delta-method

Parameters occurring in the equations of motion of an aircraft represent partial derivatives of aerodynamic force and moment coefficients with respect to the corresponding motion or control input variables. In other words these parameters can be thought of as variation in aerodynamic coefficients due to small

variable is

one of the motion or control variable about the nominal value in such a way that only that particular variable is allowed to change while rest of the variables are held constant at their nominal values. This fundamental understanding is captured in Table 1 related for calculating aircraft parameters.

Let us now assume that FNN is already trained to map the network input variables $\rho, \alpha, \beta, \delta_a$ and δ_r to the output variables \dot{C}_1 or \dot{C}_2 or \dot{C}_3 . Now only one of the network inputs is given a small/random perturbation at each time point while all others are held at their original values. Such a modified input file is now presented to the trained neural network to predict the perturbed value of aerodynamic coefficients at its output node. The difference in the predicted value of aerodynamic coefficient from the value predicted for the original values of inputs is due to the perturbation in the value of the chosen network input variable. The difference is calculated in the value of aerodynamic coefficient divided by the perturbation value gives the corresponding aircraft parameter. For example say β is perturbed by small value $\Delta\beta$ and difference observed in the predicted value of C_1 for β and $\beta+\Delta\beta$ is ΔC_1 . Then $\Delta C_1/\Delta\beta$ yields the stability derivative $C_{1\beta}$. Similarly perturbation in δ_a and corresponding ΔC_2 observed will yield control derivative $C_{2\delta_a}$, where $C_{2\delta_a} = \Delta C_2/\Delta\delta_a$. To note that due to one sided differences, motion and control variables are perturbed in both increasing and decreasing direction. For example C_3 values for $\beta+\Delta\beta$ and $\beta-\Delta\beta$ are predicted

to be $C_{y_0}^c$ and C_{y_0} respectively, then $C_{y_0}^c = C_{y_0}^c - C_{y_0}^c / \Delta \delta \delta$

It should be noted that for each of the perturbed values at each time point, there will be a corresponding perturbed value of aerodynamic coefficient, and hence a different calculated value of the parameter estimate. Ideally all such values should have been observed to yield a single value of the parameter. However in reality there is variation in predicted values. Histograms of all the estimated values showed a near normal distribution. Thus the mean value is used as the estimate and standard deviation about the mean as the measure of accuracy of the estimates.

3.3 Simulated Data Generation

In the absence of real flight data, simulated data is used as the input-output data to train the FFNN. This simulated data is obtained by solving the lateral-directional equations of motion for an example aircraft. For the present study, the example aircraft was chosen to be the DLR research aircraft ATTAS, details of which are given in the DLR report by Jategaonkar¹⁸. This aircraft was chosen as real flight data for it was acquired recently and are being analysed by others. Thus it would help comparing with results from real flight data in a later data. Also, we could obtain the control input from used for real flight and we have analysed the corresponding simulated data for parameter estimation. For generation of simulated data equations of motion used are given next:

3.4 Equations of Motion

For generation of lateral-directional simulated flight data, following perturbed equations of motion^[2] were used

$$\dot{v} = -v/U_1 + p \sin \theta + q \cos \theta \sin \phi + (\tilde{g}/24a) C_{Yp} \quad (13a)$$

$$\dot{w} = p \sin \theta + q/U_1 + q \cos \theta \cos \phi + (\tilde{g}/24a) C_{Yq} \quad (13b)$$

$$\dot{\phi} = \phi \tilde{g} \tilde{U}_1 / U_1 + (\tilde{g}^2/24a) H_1 \phi \tilde{U}_1 C_{Y1} + (\tilde{g}^2/24a) C_{Y1} + \phi \tilde{g} (\tilde{U}_1^2 + U_1^2) / U_1 + \phi \tilde{g} (U_1^2 - \tilde{U}_1^2) / U_1 + \tilde{g} \tilde{U}_1 \tilde{U}_1 \quad (13c)$$

$$\dot{r} = \phi \tilde{g} \tilde{U}_1 / U_1 + (\tilde{g}^2/24a) H_2 \phi \tilde{U}_1 C_{Y2} + (\tilde{g}^2/24a) C_{Y2} + \phi \tilde{g} (\tilde{U}_1^2 + U_1^2) / U_1 + \phi \tilde{g} (U_1^2 - \tilde{U}_1^2) / U_1 + \tilde{g} \tilde{U}_1 \tilde{U}_1 \quad (13d)$$

$$\dot{\theta} = p + q \sin \phi \tan \theta + r \cos \phi \tan \theta \quad (13e)$$

$$\dot{\psi} = q \cos \phi + r \sin \phi \quad (13f)$$

where,

$$\tilde{g} = v/U_1 \quad \tilde{U}_1 = (g/U_1^2)^{1/2} \tilde{g}$$

$$C_{Y1} = C_{Yp}(\phi b/24U_1) + C_{Yq}(\phi b/24U_1) + C_{Y\dot{\phi}}\dot{\phi} + C_{Y\dot{\theta}}\dot{\theta} + C_{Y\dot{\psi}}\dot{\psi} \quad (14a)$$

$$C_{Y2} = C_{Yp}(\phi b/24U_1) + C_{Yq}(\phi b/24U_1) + C_{Y\dot{\phi}}\dot{\phi} + C_{Y\dot{\theta}}\dot{\theta} + C_{Y\dot{\psi}}\dot{\psi} \quad (14b)$$

$$C_{Y3} = C_{Yp}(\phi b/24U_1) + C_{Yq}(\phi b/24U_1) + C_{Y\dot{\phi}}\dot{\phi} + C_{Y\dot{\theta}}\dot{\theta} + C_{Y\dot{\psi}}\dot{\psi} \quad (14c)$$

The steady flight conditions, which the perturbations are initiated, mass, moment of inertia, and geometric measures of the aircraft, taken from reference^[2], are as follows :

$$U_1 = 185.0 \text{ m-sec}^{-1}$$

$$M = 1652.25 \text{ kg}$$

$$g = 9.81 \text{ m-sec}^{-2}$$

$$\rho = 1.225 \text{ kg m}^{-3}$$

$$S = 64 \text{ m}^2$$

$$c = 3.059 \text{ m}$$

$$b = 21.5 \text{ m}$$

$$\begin{aligned} I_{xx} &= 162332.2 \text{ kg-m}^2 & I_{xy} &= 202637.9 \text{ kg-m}^2 \\ I_{yy} &= 281645.99 \text{ kg-m}^2 & I_{zz} &= 11442.9 \text{ kg-m}^2 \end{aligned}$$

where U_0 is the velocity, ρ is density of winging aircraft of aircraft under consideration, b is the span, \bar{c} is mean aerodynamic chord, S is reference area and x_i are the moment of inertia about the principal axes.

Fourth order Runge-Kutta method is used to solve above set of equations for generating matrix variables $\phi(t), \theta(t), \psi(t)$ for some known control input form of δ_{ail} and δ_{ail} . The network input file is prepared using these values of ϕ, θ, ψ and $\dot{\phi}, \dot{\theta}, \dot{\psi}$. The force and moment coefficient $C_L, C_D, C_Y, C_{L\dot{\phi}}, C_{D\dot{\theta}}, C_{Y\dot{\psi}}$ are calculated from eq (14a-14e) and these form network output variables for simulated flight data. True values of the parameters given in Table 1 were fed into the above set of equations (14a-14e).

CHAPTER 4

RESULTS AND DISCUSSION

Results and Discussion

Simulated flight data for lateral-directional dynamics of an aircraft were generated for different combinations of column and rudder control inputs. The network input file consisted of motion variables $[p, r, \delta]$ along with aircraft control inputs δ_a and/or δ_r . The network output file was either $C_{l\delta}$ or $C_{y\delta}$ or $C_{n\delta}$. The network was trained using such input-output files for many such sets of simulated flight data. The network tuning parameters were varied to obtain the optimal architecture that was used for parameter estimation for all the sets of flight data. To this purpose network parameters were varied in the range shown below. The final values selected for the present study are also shown below in the third column.

Network Parameter	Range of variation tried	Final Value
Logistic Gain	0.05-1.0	0.05
Random Seed	0.0-0.9	0.4
Number of Hidden Layers	1-3	1
Number of Nodes in Hidden Layer	4-10	4
Number of Iteration	2000-10000	5000
Learning Rate	0.0-0.4	0.3
Momentum Rate	0.0-0.8	0.5

The criterion for selection of network parameters was based on MSE observed at the end of selected number of iterations. It was found that MSE decreased up to about 5000 iterations, and beyond it the decrease was marginal. To save on computational

now, for all the further studies the architecture along with number of iterations was kept fixed at 1000. Although it is possible that slight variations in the network parameters may result in lower MSE for specific set of flight data it was decided to freeze the architecture of network for all studies reported herein due to limitation of time. Since present work is concerned with parameter estimation via Delta-method, we refrain from reporting detailed discussion on training phase and effects of network parameters on the MSE and thereby on the match obtained between the desired and the predicted values of C_L or C_D or C_p . The effect of network parameters on training was similar to that reported in the literature, i.e., Bhanuprakash and Jagannathan²⁴ and Rajesh Kumar¹².

As reported in literature, multistep 3-2-1-1 type of control inputs have been found very efficient for generation of flight data to be used for parameter identification. A multistep 3-2-1-1 type of input consists of control deflection for 3,2,1 and 1 second in α , α , α , α and α direction respectively. The maximum magnitude was kept at 0.2 or 0.05 radians, and duration was seven seconds. To bring out the relative merits of 3-2-1-1 type of input, it was of interest to explore parameter estimation using flight data for other type of control inputs. Two such control inputs, namely an arbitrary and a sinusoidal (Fig.6) were used for flight data generation. For such a comparative study following five types of control inputs were used to obtain corresponding flight data for parameter estimation via Delta-method.

- case I : White-noise 3-D-a-1 sensor input, maximum amplitude 0.1 radians and duration seven seconds.
- case II : White-noise 3-D-a-1 rudder input, maximum amplitude 0.1 radians and duration seven seconds.
- case III : An arbitrarily varying sensor control input with maximum amplitude 0.1 radians and duration seven seconds.
- case IV : A sinusoidal sensor input of maximum amplitude 0.1 radians and duration seven seconds.
- case V : Combination of step-and-ramping multi-step 3-D-a-1 sensor and rudder control inputs. Both having maximum amplitude as 0.1 radians and duration seven seconds.

Using these different inputs, the simulated flight data was generated and parameters were predicted via Delta-method. The results corresponding to case I - V are listed respectively in columns 3 - 7 of Table 1, along with true values of parameters in column 8 for ready comparison.

case I (Table 1, column 3) : As seen from Table 1, except for C_{yp} and C_{yr} all the other parameters are well estimated. However, values of standard deviation for some of the parameters are on higher side. Further, control derivatives like $C_{l\delta r}$, $C_{n\delta r}$, $C_{p\delta r}$ cannot be estimated since there is no rudder input available in the sensor's input file for perturbation as required by Delta method.

case II (Table 1, column 4) : Results for δr alone show degradation as compared to those for δa alone. Comparison with 3rd

column four it shows that, in addition to C_{yp} , C_{yr} in case 1, C_{xp} , C_{xr} and C_{yr} are also poorly estimated. Again, control derivatives for values $(C_{\dot{y}_{in}}, C_{\dot{y}_{out}}, C_{\dot{y}_{in}})$ can not be estimated for this data, since no \dot{y}_a is available in network input file.

case III (Table 1, column 5) : Compared to case 1, the arbitrary \dot{y}_a control input results showed degradation in estimated values, specially in C_{xp} , C_{xp} and C_{yr} values while C_{yp} and C_{yr} estimates remained poor as in case 1. Thus injecting 2-D-1-1 input signal shows its superiority over the arbitrary input signal.

case IV (Table 1, column 6) : The parameter estimates were poor except for derivatives $(C_{\dot{y}_{in}}, C_{\dot{y}_{out}}, C_{\dot{y}_{in}})$ as compared to the cases discussed above. This is due to the fixed frequency of the sinusoidal signal which is unable to excite all the modes of the aircraft dynamics.

case V (Table 1, column 7) : All the above cases had only one of the controls (\dot{y}_a or \dot{y}_r) used for exciting aircraft's dynamics, and thereby we could estimate only the corresponding control derivatives, i.e., either \dot{y}_a or \dot{y}_r . Simultaneous, identical \dot{y}_a and \dot{y}_r inputs were used for generating flight data and as control derivatives for both \dot{y}_a and \dot{y}_r could be estimated by perturbing them in network input file. Estimates from this data showed that, like previous cases, C_{yp} and C_{yr} were still being poorly estimated and estimates for both \dot{y}_a and \dot{y}_r $(C_{\dot{y}_{in}}, C_{\dot{y}_{out}}, C_{\dot{y}_{in}}, C_{\dot{y}_{out}}, C_{\dot{y}_{in}}, C_{\dot{y}_{in}})$ were also poor. A close scrutiny of the estimated values of these control derivatives showed that there was a pair-wise high correlation between $(C_{\dot{y}_{in}}, C_{\dot{y}_{in}})$.

$(\partial C_{\text{Lift}}/\partial C_{\text{Pitch}})$ and $(\partial C_{\text{Lift}}/\partial C_{\text{Roll}})$ in the sense that both the control derivatives of the pair had almost equal values. Initially this result looked very strange but on reflection, it was clear that indeed the values should be either exactly equal or almost equal as was the case. The reason for expecting such equal estimates for both is that we are showing the neural network two identical inputs namely, $\delta\alpha$ and $\delta\beta$, but they are indistinguishable from neural network point of view. It is like showing the same input twice to neural network.

The above observation required a rethink as the type of control inputs to be used for generating flight data as as to enable estimation of all the stability and control derivatives with better accuracy. As a first step we used the real control inputs that has been used in generating real flight data provided by B&B Germany. We could not analyse the whole set of this real flight data as these were received very late when the thesis work was nearing completion. Analysis of complete data set is being carried out by another Ph.D. candidate.

From the data set supplied we chose two types of control inputs form which are put under case VI and case VII.

case VI : Pulse type elevator input (Fig.5)

case VII : Continuous sinusoidal 0-2-1-1 type elevator and rudder inputs (Fig.6a and 6b)

Using these control inputs, simulated data was generated and parameters estimated via Delta-method. The results for these two cases are given in table 3 and discussed below.

case VI (Table 2, column 3) – In general, the estimated parameters compared well with the true values, except that the rubber control derivatives still could not be estimated and derivatives like $C_{\dot{\delta}_r}$, $C_{\dot{\delta}_r'}$ and $C_{\dot{\delta}_r''}$ were not well estimated.

case VII (Table 2, column 4) – Estimated parameters in this case showed remarkable improvement in their estimated values when compared with case V. Here not only were both control derivatives estimated separately but also their estimated values were close to the true values and standard deviations were reasonably low. On the whole, all the parameter estimates showed better comparison with the true values.

On the face of it, such improved results were surprising and it was first suspected that this could be due to measurement noise that may be present in the control inputs copied out from the real flight data. Alternatively, it was conjectured that this may be due to the rubber and silver inputs being not identical as was the case for case V. Thus, the real control inputs may have contained measurement noise and would not have identical shape. To test this conjecture, flight data was generated for δ_a and δ_r combination where both δ_a and δ_r inputs had certain periodic measurement noise added to them. Specifically periodic measurement noise of 10 and 50 was added to the control inputs that were used in case V i.e. combination of manitrop 3-2-0-0 δ_a and δ_r . The estimated parameters from each flight data are discussed below:

case VIII (Table 2, column 5) – Combination of manitrop 3-2-0-0 δ_a and δ_r with 10 measurement.

noise in δu and δv

The estimated parameters did not show any improvement over that estimated in case V. The estimated values of post-syst control derivatives still showed trend similar to the one obtained under case V.

case IX (Table 2, column 6) : Combination of manuever 2-2-1-1

δu and δv with 25 measurement noise

in δu and δv

Estimated parameters still followed the same trend as their estimated values as in case VII.

At this stage, difficulty of estimating control derivatives when combination of δu and δv is used led to idea of introducing delay between the two control inputs. As mentioned earlier, identical control inputs δu and δv would confuse the neural network and it would not be able to distinguish between δu and δv inputs. It was hoped that the delay would give a chance to neural network to distinguish between these two control inputs i.e. δu and δv . Based on this conjecture, following types of inputs were used for data generation and analysis, results of which are given in table 3

case X (Table 3, column 3) : Combination of manuever 2-2-1-1 δu

and δv with rubber control delayed by
1.0 second i.e. rubber input was
initiated 1 second after aileron
input is applied

The estimated parameters clearly reflected the success of

time delay between the two inputs but only the control derivatives got measured but also were very close to their true values ($C_{y\delta_R}$ being only exception) and with reasonable low standard deviation. However, stability derivatives $C_{\dot{\omega}_x}$, $C_{\dot{\omega}_y}$, $C_{\dot{\omega}_z}$ and $C_{\dot{\omega}_p}$ were still on higher scale. It seemed desirable to explore and find control input form that might reduce these measured deviations.

case XI (Table 3, column 4) : Continuation of multistep 3-2-1-1 δ_R and δ_r with sensor control delayed by 1.0 second.

Like case X, parameters were again well estimated except for some derivatives as $C_{y\delta_R}$ and $C_{\dot{\omega}_p}$ values.

case XII (Table 3, column 5) : Continuation of multistep 3-2-1-1 δ_R and δ_r with rudder control delayed by 2.0 second.

Estimated parameters from this study yielded good estimated values for all derivatives except $C_{\dot{\omega}_x}$, $C_{\dot{\omega}_p}$ and $C_{\dot{\omega}_z}$. Overall the 2.0 second delay was rather impressive as 1.0 second delay.

In the light of the potential shown by time delay between the applications of the two control inputs, the idea was further extended wherein second control followed at the end of the first control. The following two cases were investigated towards this goal:

case XIII (Table 4, column 2) : Continuation of multistep 3-2-1-1 δ_R and δ_r such that reference input was applied for the first seven

seconds, rubber input kept zero
 and for the next seven seconds
 rubber input being applied keeping
 silicon input zero

case XIV (Table 4, column 4) : Combination of instepest 3-2-3-1 As
 and for each test rubber input is
 applied for the first seven seconds
 and silicon input for the last
 seven seconds.

The estimated parameters from case XII and XIV, clearly
 indicate that for each type of control inputs, their values are
 suitable for neural network. It can very easily distinguish
 between two inputs. It was also observed that in case XIV the
 standard deviations were much lower than the above type of
 application of control inputs resulted in good estimation of even
 the weak derivatives like $C_{xy}/C_{yz}/C_{yz}/C_{yz}/C_{yz}$ and C_{yz} .

For illustration, specifically for case XII, the actual, the
 trained and the predicted values of $C_{xy}C_{yz}/C_{yz}$ are plotted in
 Fig 3a, 3b, and 3c. By actual value we mean those values of force
 or moment coefficients which were calculated using eq(14) with
 true values of parameters for particular control input of case
 XII. As values of Dase force or moment coefficients were provided
 as output in the input-output file used to train the ITNN, the
 values as obtained after training the ITNN for optimal network
 parameters are termed as trained values. The predicted values are
 those values which are obtained by using all the estimated
 parameters as eq(14). It may be seen from Fig. 7 that the actual,

calculated and predicted $C_{L0}C_{L0}$ and C_{L0} their good match, and thus indicate validation of Extra method for predicting posterior estimates for flight data.

Also histograms for all the estimated parameters are plotted in Fig. 19,20 and 21. These figures clearly indicate the near normal distribution for most of the estimated parameters and justify the concept of mean values and standard deviation for these estimated parameters.

Since the real flight data is generally noisy in nature the effect of measurement noise on the estimated parameters was carried out to show how the accuracy of the estimates is affected by presence of measurement noise. For this purpose pseudo measurements noise was added to μ, r, δ and C_{L0} or C_{L0} or C_{L0} corresponding to simulated flight data of case 2. The results for it are given under case XV and case XVI below :

case XV (table 4, column 10) : case 2 + 1% measurement noise in

$$\mu, r, \delta \text{ and } C_{L0} \text{ or } C_{L0} \text{ or } C_{L0}$$

case XVI (table 4, column 11) : case 2 + 5% measurement noise in

$$\mu, r, \delta \text{ and } C_{L0} \text{ or } C_{L0} \text{ or } C_{L0}$$

In case XV most of the parameters are well estimated as was observed for case 2 (no noise). This indicates that presence of low measurement noise does not affect the accuracy of estimates and this reflects on the robustness of Extra-method. A comparison of results for 1% (case XVI) and 5% (case XVII) cases shows the increase in noise level does result in marginally poorer estimates for most of the parameters. Conversely, some of the cross derivatives like $C_{L0\mu}$, C_{L0r} and $C_{L0\delta}$ are actually better estimated.

CHAPTER 5

CONCLUSIONS AND RECOMMENDATIONS

5.1 Conclusions

In the present work, Delta method using RTN6 has been used for estimation of lateral-directional parameters from simulated flight data. Different types of control inputs were used to generate corresponding sets of flight data for analyses through Delta method. Comparisons of parameter estimates as obtained showed that the accuracy of estimates depends on the types of control input used for flight data. In particular, it was observed that a time delay between aileron and rudder inputs leads to better estimates of aileron and rudder control derivatives. Further, multiway 3-2-1-1 type aileron and rudder lead to better estimates of aircraft dynamics and thereby to better estimates as compared to pulse, sinusoidal or any arbitrary varying input. The Delta method has been found to be robust enough to provide good parameter estimates even in presence of measurement noise in the flight data.

5.2 Recommendations

It would be of great interest to validate Delta method on real flight data, in particular if data could be generated for different types of control inputs studied in the present work, then these could be readily compared to the results reported herein. The effect of time delay between aileron and rudder inputs is worth verifying using real flight data. In present work, force and moment coefficients have been mapped separately, it would be

attempting to minimize where C_1, C_2 and C_3 are mapped together and then apply Delta method for parameter estimation.

REFERENCES

1. Smith, E., and Morris, J. J. "The Stability Derivatives of the T-6A Aircraft Estimated by Various Methods and Derived from Flight Test Data," FAD-ED-75-4
2. Smith, E., "Stability and Control of Airplanes and Helicopters," Academic Press, New York, 1964
3. Edwards, D.E., "X-28B Stability and Control Hand Book (DATCOM 1)," Wright Patterson Air Force Base, OHIO, Revised August 1968
4. Morris, R. E. and Jeff, E. W., "Identification of Dynamic Systems - Theory and Formulation," NASA, SP 103 Feb. 1970.
5. Pearson, A. "Identification of Aerodynamic Derivatives of the F4D OF F4D Aircraft from Flight Test by means of Neural Analog Model Matching," Paper No. F4D-F4D2 at Publication ESDP-77-084, Nov. 1979
6. Taylor, L. W., Jeff, E. W., and Powers, B. G.'s comparison of Newton-Raphson and other Methods for Determining Stability Derivatives from Flight Data,⁸ AIAA, Paper No. 45-615, May 1965
7. Kim, V. "Identification Evaluation Methods," OASD-LE-104, Nov. 1979
8. Fodor, B., "20 Years of Adaptive Neural Networks: Perceptrons, Machines and Backpropagation," Proceedings of the IEEE, Vol. 78, No. 5, Sep. 1990, pp. 1429-1441
9. Chao, S., Cowan, C. P. R., "Parallel Networks Prediction

10. Chen, B., Billings, S. A. and Grant, P. M., "Nonlinear System Identification Using Neural Networks," *Int. J. Control*, 1990, Vol. 51, No. 4, pp. 1219-1234.
11. Sjöberg, J., Rudenstrom, R. and Ljung, L., "Neural Networks in System Identification," *Proceedings of the 1994 IFAC Symposium on System Identification*, 4-6 July 1994, Copenhagen, Denmark, Vol. 2, pp. 49-54.
12. Hays, R. A., "On the Use of Backpropagation with Feed Forward Neural Networks for the Aerodynamic Estimation Problem," AIAA-93-0628-CP, 1993.
13. Yousefi, H.M., "Estimation of Aerodynamic Coefficients using Neural Networks," AIAA paper 93-0618, Aug. 1993.
14. Saegusa and Jirapongchar, B. V., "Aspects of Feed Forward Neural Network Modeling and its Application to Lateral - Directional Flight Data," *DLA 88-05-020*, Sep. 1988.
15. Bass, J. B. and Jirapongchar, B. V., "Aircraft Parameter Estimation Using Recurrent Neural Networks - A critical appraisal," AIAA Paper 93-0604-2, Aug. 1993.
16. Linn, D. J., and Saegusa, B. P., "Modification of Aerodynamic Coefficients Using Computational Neural Networks," *Journal of Guidance Control and Dynamics*, Vol. 16, No. 4, Nov-Dec 1993, pp. 1028-1035.
17. Ruckenstein, S.C., Ghosh, S.R. and Kuhn, P.R. "Two New Techniques for Aircraft Parameter Estimation Using Neural

Manuscript (submitted for publication)

16. Jengender R. "Identification of The Aerodynamic Model of The SBR Research Aircraft ATD6 From Flight Test Data" DLR -P89-40, Sept. 1989
17. Rakesh Kumar . "Parameter Estimation From Flight Data Using Feed Forward Neural Networks" M Tech Thesis Aerospace Engg Department, IIT-Kanpur, February '94

TABLE 1

Parameter	True Value	Estimated Parameters				
		case1	case2	case3	case4	case5
$-C_{sp}$	0.90	[-]	0.77	0.88	0.90	0.92
		10.181	10.120	10.881	10.181	10.181
C_{sp}	0.40	0.40	0.44	0.44	-0.17	0.58
		10.121	10.873	10.121	10.281	10.281
$-C_{sd}$	0.128	0.098	0.101	0.148	0.10	0.11
		10.0281	10.021	10.030	10.0340	10.023
$-C_{ls}$	0.20	0.24	NE	0.20	0.13	0.094
		10.081		10.041	10.053	10.001
C_{lsr}	0.048	NE	0.044	NE	NE	-0.90
			10.0120			10.0291
$-C_{sp}$	0.105	0.14	0.84	0.03	0.04	0.10
		10.041	10.391	10.051	10.031	10.091
$-C_{sr}$	0.408	0.44	0.77	0.12	0.24	0.48
		10.170	10.123	10.181	10.221	10.150
C_{sp}	0.38	0.38	0.38	0.19	0.21	0.38
		10.041	10.051	10.070	10.041	10.051
C_{sdls}	0.0	0.001	NE	-0.004	0.003	-0.077
		10.0031		10.0043	10.0003	10.021
$-C_{lsr}$	0.14	NE	0.14	NE	NE	-0.08
			10.021			10.021

C_{pe}	0.340	0.442	0.193	0.19	0.47	-0.000
		(0.19)	(1.39)	(0.21)	(0.17)	(0.04)
C_{pr}	0.722	0.83	0.80	-0.20	0.70	0.21
		(1.89)	(0.40)	(1.03)	(0.91)	(0.85)
$-C_{pb}$	1.132	0.18	0.12	0.84	0.95	1.1
		(0.34)	(0.34)	(0.30)	(0.30)	(0.15)
C_{pba}	0.03	0.034	NE	0.024	0.07	0.045
		(0.01)		(0.03)	(0.03)	(0.08)
C_{ptr}	0.09	NE	0.14	NE	NE	0.12
			(0.02)			(0.04)

SE = standard deviation.

NE = not estimated

Table 2

Parameter	True Value	Estimated Parameters			
		case6	case7	case8	case9
$-C_{1p}$	0.98	1.1 (0.113) ^{SE}	0.91 (0.111)	0.93 (0.131)	0.93 (0.131)
C_{1p}	0.42	0.43 (0.073)	0.41 (0.121)	0.38 (0.171)	0.38 (0.221)
$-C_{1g}$	0.128	0.088 (0.031)	0.121 (0.031)	0.11 (0.038)	0.18 (0.031)
$-C_{1gs}$	0.22	0.23 (0.041)	0.253 (0.041)	0.281 (0.031)	0.28 (0.031)
C_{1dr}	0.048	NE	0.21 (0.341)	0.281 (0.321)	0.09 (0.0361)
$-C_{1p}$	0.118	0.18 (0.081)	0.25 (0.131)	0.19 (0.081)	0.19 (0.081)
$-C_{2p}$	0.493	0.58 (0.181)	0.64 (0.191)	0.69 (0.181)	0.49 (0.171)
C_{2g}	0.28	0.27 (0.081)	0.38 (0.091)	0.34 (0.081)	0.26 (0.081)
C_{2gs}	0.0	-0.003 (0.0031)	0.003 (0.0041)	-0.071 (0.031)	-0.073 (0.031)
$-C_{2dr}$	0.14	NE	0.18 (0.041)	-0.078 (0.031)	-0.082 (0.0341)

C_{2P}	0.34	0.34	0.34	-0.003	-0.003
		(0.04)	(0.03)	(0.04)	(0.04)
C_{2F}	0.127	1.13	0.30	0.17	0.28
		(0.4)	(0.03)	(0.03)	(0.04)
$-C_{2B}$	1.133	0.97	1.07	0.1	1.1
		(0.09)	(0.03)	(0.03)	(0.04)
C_{2Ba}	0.02	0.02	0.028	0.046	0.055
		(0.03)	(0.04)	(0.04)	(0.04)
C_{2Br}	0.18	0.0	0.19	0.12	0.12
			(0.04)	(0.04)	(0.04)

SE = standard deviation

RE = roi returned

c_{y^*}	0.30	0.34	0.34	0.000	0.000
		10.140	10.030	10.040	00.040
c_{y^*}	0.929	1.13	0.20	0.07	0.20
		10.01	10.01	10.051	10.040
$-c_{y^*}$	1.130	0.07	1.00	0.1	1.1
		10.010	10.031	00.001	10.050
c_{y^*}	0.03	0.05	0.000	0.000	0.000
		10.000	10.041	00.001	10.000
c_{y^*}	0.10	00.	0.15	0.10	0.10
			10.001	00.041	0.001

0 = standard deviation

00 = not calculated

Table 3

parameter	True Value	Estimated Parameters		
		case10	case11	case12
$-C_{1P}$	0.98	1.07 (0.88) ⁰	1.02 (0.84)	0.93 (0.72)
C_{1P}	0.42	0.43 (0.88)	-0.38 (0.83)	0.37 (0.87)
$-C_{1B}$	0.126	0.12 (0.83)	0.12 (0.82)	0.12 (0.816)
$-C_{1Bz}$	0.12	0.28 (0.84)	0.28 (0.84)	0.24 (0.83)
$-C_{1Bx}$	0.046	0.04 (0.812)	0.042 (0.816)	0.042 (0.816)
$-C_{2P}$	0.112	0.10 (0.84)	-0.043 (0.88)	0.08 (0.88)
$-C_{2B}$	0.498	0.55 (0.85)	0.22 (0.83)	0.48 (0.82)
C_{2B}	0.38	0.38 (0.84)	0.38 (0.84)	0.27 (0.84)
C_{2Bz}	0.0	0.868 (0.83)	0.884 (0.834)	-0.009 (0.816)
$-C_{2Bx}$	0.18	0.18 (0.83)	0.18 (0.83)	0.20 (0.83)

C_{2P}	0.30	0.25	10.025	0.166
		10.291	10.340	10.179
C_{2T}	0.120	0.73	-0.34	0.53
		10.321	10.870	10.41
$-C_{2B}$	1.132	1.84	1.07	1.83
		10.171	10.243	10.171
C_{2Ba}	0.03	0.911	0.034	0.534
		10.041	10.025	10.001
C_{2Br}	0.19	0.18	0.22	0.243
		10.081	10.11	10.081

σ = standard deviation

Table 1: 4

Parameter	True Value	Estimated Parameters			
		case13	case14	case15	case16
$-C_{top}$	0.99	1.00 (0.11) ⁹⁹	0.99 (0.00)	1.00 (0.15)	1.00 (0.20)
C_{LF}	0.42	0.39 (0.08)	0.42 (0.03)	0.44 (0.08)	0.51 (0.30)
$-C_{LB}$	0.128	0.12 (0.02)	0.12 (0.004)	0.12 (0.01)	0.1 (0.04)
$-C_{LH}$	0.29	0.26 (0.03)	0.28 (0.007)	0.28 (0.04)	0.23 (0.04)
C_{LFR}	0.046	0.045 (0.001)	0.047 (0.003)	0.04 (0.013)	0.05 (0.03)
$-C_{op}$	0.115	0.12 (0.07)	0.12 (0.04)	0.101 (0.14)	0.095 (0.13)
$-C_{or}$	0.405	0.54 (0.06)	0.33 (0.11)	0.49 (0.14)	0.47 (0.14)
$-C_{op}$	0.28	0.28 (0.03)	0.27 (0.05)	0.26 (0.04)	0.27 (0.04)
C_{phs}	0.0	-0.001 (0.001)	0.00 (0.00)	0.008 (0.003)	0.008 (0.002)
$-C_{phr}$	0.14	0.17 (0.018)	0.19 (0.04)	0.18 (0.03)	0.14 (0.02)

C_{20}	0.30	0.34	0.36	0.34	0.35
		(0.14)	(0.15)	(0.21)	(0.20)
C_{21}	0.327	0.30	0.40	0.45	0.39
		(0.10)	(0.13)	(0.23)	(0.20)
$-C_{22}$	1.132	1.11	1.11	1.08	1.03
		(0.09)	(0.11)	(0.17)	(0.17)
C_{23a}	0.60	0.007	0.003	0.004	0.03
		(0.004)	(0.008)	(0.04)	(0.003)
C_{23b}	0.19	0.31	0.19	0.10	0.19
		(0.03)	(0.02)	(0.09)	(0.06)

0 = standard deviation

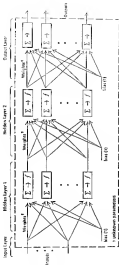


Fig. 2. Feed forward neural network with two hidden layers

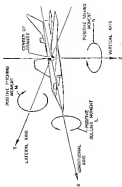


FIG. 3. Aircraft Mass System

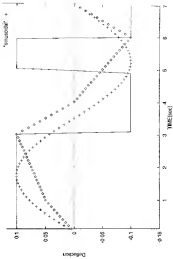


FIG. 4 Three Types of Control Input Forms

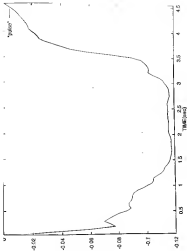


Fig. 8. Pattern used control inputs, Issue 811

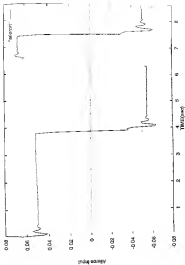
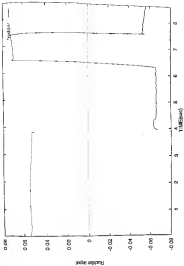


Fig. 10a and 10b: 0-0-0-0 radar input signal (from 9112)



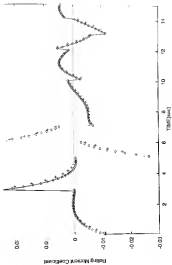


Fig. 2a Comparison of actual, Trained and estimated responses of Poling Member Coefficient ($\alpha_{1,p}$)

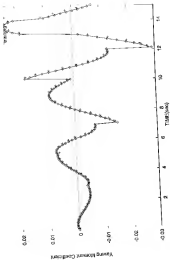


Fig. 76 Comparison of Actual, Predicted and Estimated
 Modulus of Testing Material (Coefficient 0.001)

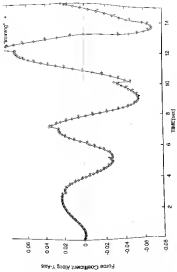


Fig. 20 Comparison of Actual, Trained and Estimated Responses of First-Order System Along With Step



Fig. 8 - Histograms for Estimated Parameters C_{pp} , C_{gr} , C_{dp} , C_{ga} , C_{gr} and C_{gd} .

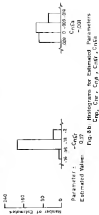
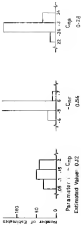


Fig. 8b Histograms for Estimated Parameters: C_{np} , C_{nr} , $C_{np}C_{nr}$

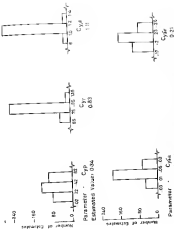


Fig. 8c: Histograms for Estimated Parameters C_{yp} , C_{yt} , C_{ypa} , C_{yfa} and C_{yfi} .

